Contrib Mineral Petrol (2005) 149: 699–712
DOI 10.1007/s00410-005-0676-5

ORIGINAL PAPER

Johannes Glodny · Uwe Ring · Alexander Kühn
Philipp Gleissner · Gerhard Franz

Crystallization and very rapid exhumation of the youngest Alpine eclogites (Tauern Window, Eastern Alps) from Rb/Sr mineral assemblage analysis

Received: 23 November 2004 / Accepted: 7 April 2005 / Published online: 24 May 2005

Abstract Multimineral Rb/Sr internal isochrons from eclogite facies rocks of the Eclogite Zone (Tauern Window, Eastern Alps) consistently yield an Early Oligocene age of 31.5 ± 0.7 Ma. This age has been obtained both for late-prograde, dehydration-related eclogitic veins, and for rocks variably deformed and recrystallized under eclogite facies conditions (2.0–2.5 GPa, 600°C). Initial Sr-isotopic equilibria among all phases indicate absence of significant post-eclogitic isotope redistribution processes, therefore the ages date eclogite facies assemblage crystallization. Equilibria also prove that no prolonged pre-eclogite facies history is recorded in the rocks. Instead, subduction, prograde mineral reactions, and eclogitization proceeded rapidly. Fast exhumation immediately after eclogitization, with minimum rates > 36 mm/a is inferred from a 31.5 ± 0.5 Ma internal mineral isochron age of a post-eclogitic greenschist facies vein assemblage. Such rates equal typical subduction rates. Late Eocene to Early Oligocene subduction of the European continental margin, with subsequent rapid exhumation of high-pressure nappe complexes has previously been recognized only in the Western Alps. The new data signify synchronous continental collision all along the Alpine belt. Our results demonstrate the unique potential of Rb/Sr assemblage 'system analysis' for precise dating of both eclogite facies and post-eclogitic events, thus for precisely constraining exhumation rates of deep-seated rocks, and for straightforward linkage of petrologic evidence with isotopic ages.

Keywords Eclogite · Rb/Sr · Geochronology · Fluid-rock interaction · Exhumation · Eastern Alps

Communicated by J. Hoefs

J. Glodny (✉)
GeoForschungsZentrum Potsdam,
Telegrafenberg C2, 14473 Potsdam,
Germany
E-mail: glodnyj@gfz-potsdam.de
Tel.: +49-331-2881375
Fax: +49-331-2881370

U. Ring · A. Kühn
Institut für Geowissenschaften,
Johannes Gutenberg-Universität,
Becherweg 21, 55099 Mainz,
Germany

P. Gleissner · G. Franz
Institut für Angewandte Geowissenschaften,
TU Berlin, Ernst-Reuter-Platz 1, 10587 Berlin,
Germany

Introduction

Isotopic dating of eclogite facies metamorphism is of key importance for understanding the dynamics of subduction zone and continental collision processes, but is difficult for various reasons. Metamorphic zircon, sometimes present mainly as overgrowths on inherited grains, occasionally allows application of in situ U/Pb methods, an approach on which most reported successful attempts at high-precision dating are based. However, it is commonly not straightforward to demonstrate zircon growth at peak eclogite facies conditions. In the absence of demonstrably eclogitic zircon, geochronology has to rely on radioactive decay systems in other eclogite facies phases. Ar-based dating is often compromised by unpredictable amounts of excess and/or inherited Ar, but may be useful in the context of multisystem geochronology (e.g., Li et al. 1994; Arnaud and Kelley 1995; Jahn et al. 2001). Sm/Nd and Lu/Hf are important chronometers as these methods potentially facilitate direct dating of eclogitic garnet growth. However, both Sm/Nd and Lu/Hf garnet-based eclogite dating can yield geologically meaningless ages due to isotopic disequilibria related to inclusions in garnet, or due to inclusion-related disequilibria or incomplete isotopic rehomogenization during metamorphism (e.g., Thöni and Jagoutz 1992; Blichert-Toft and Frei 2001).

The potential of Rb/Sr isotopic data for eclogite geochronology is almost unexploited. Phengite Rb/Sr data were used, in combination with whole rock data or

data for another phase, to calculate "cooling ages" following the concepts of Dodson (1973). This approach is not capable of recognizing intra- or intermineral isotopic disequilibria, which would invalidate age constraints. Furthermore, numerous studies challenge the general applicability of the closure temperature concept (Giletti 1991; Villa 1998 and references therein; Kelley and Wartho 2000; Kühn et al. 2000; Jenkin et al. 2001; Glodny et al. 2003) by showing that the isotope budget of a mineral grain depends not only on temperature but is also governed by the isotope transport properties of the polymineralic assemblage and of grain boundaries in the rock matrix surrounding it. Thus, the geochronologic meaning of phengite-based two-point isochrons often remains obscure.

Further, it is widely perceived that the Rb/Sr system is susceptible to open-system behaviour and resetting. In fact, Rb and Sr are generally mobile in aqueous intergranular fluids. In metamorphic rocks, conditions like deformation–recrystallization processes, long-term persistence of high temperatures, and mineral reactions in the presence of fluids which involve Rb, Sr-bearing minerals, will lead to Rb and Sr redistribution, with either partial or complete textural, physico-chemical, and isotopic equilibration. Textural disequilibria are commonly associated with Sr-isotopic disequilibria among minerals (cf. Vance et al. 2003), which widely compromise isotopic dating by the Rb–Sr method. In contrast, textural and physico-chemical equilibrium is a good indicator for preserved or achieved initial Sr-isotopic equilibrium, which is a pre-requisite for successful age determination. Depending on the size of equilibrated domains, the method of choice for separation of minerals for dating is either Rb/Sr microsampling using a microdrill (Müller et al. 2003 and references therein; Cliff and Meffan-Main 2003;

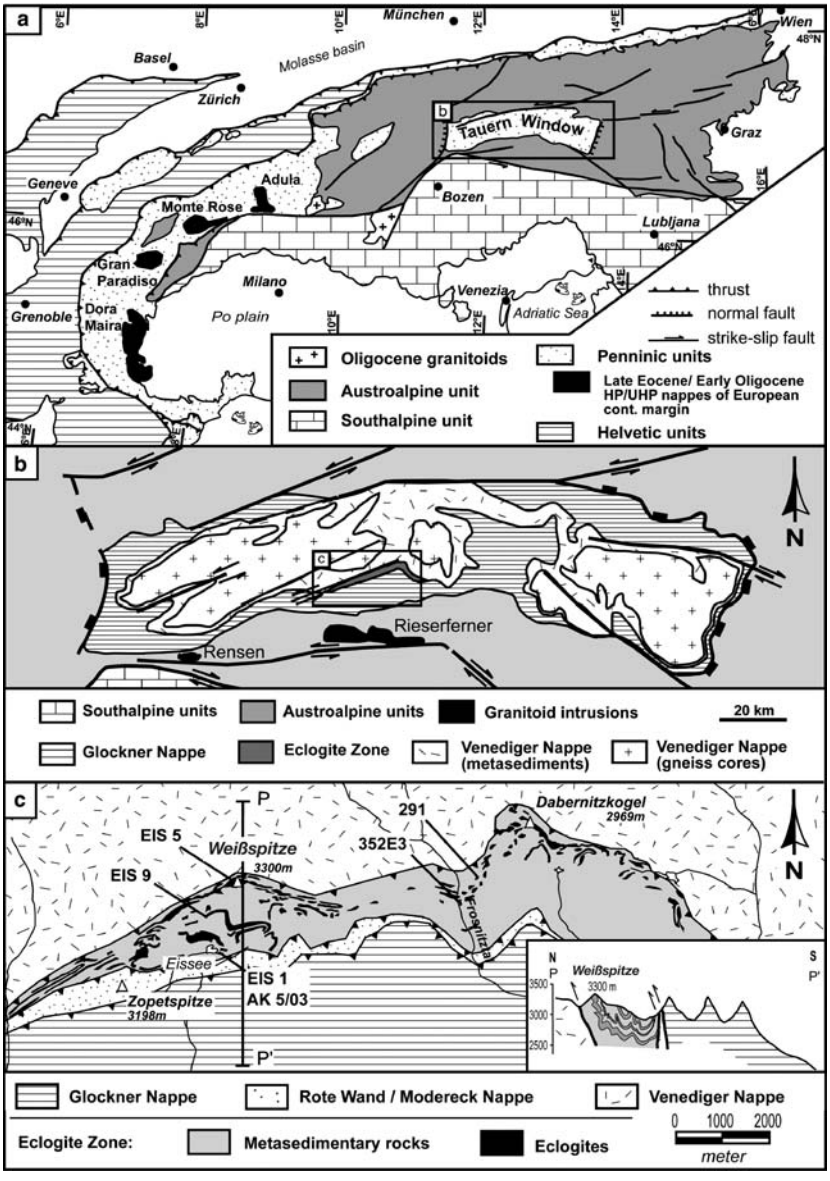

Fig. 1 Geological and tectonic sketch maps. **a** Location of the Tauern Window within the Alpine belt. **b** Tectonic map of the Tauern Window area (modified from Frisch et al. 2000). *Box* indicates position of the Eclogite Zone. **c** Map of the Eclogite Zone and adjacent units, with sample locations. Eclogite is outlined in *black*. Map base: Geologische Karte der Republik Österreich, 1:50000, Blatt 152 Matrei, 1987. Inset profile after Raith et al. (1980)

Meffan-Main et al. 2004) or bulk mineral separation from carefully selected small (cm-size) samples (Glodny et al. 2003).

The geological significance of Rb/Sr mineral ages crucially depends on whether Sr-isotopic equilibrium among different phases had been achieved during the process to be dated and was modified later only by in situ radioactive decay. As textural and chemical equilibrium does not always ensure isotopic equilibrium (Cliff and Meffan-Main 2003), verification of initial isotopic equilibrium is necessary and requires Rb/Sr analysis of different phases, followed by correction for in situ radiogenic ingrowth of ^{87}Sr. This approach is inherently flawed by the propagation of analytical uncertainties into the calculation of initial $^{87}Sr/^{86}Sr$ ratios, but it still detects any significant non-analytical variability. We therefore consider an assemblage as initially equilibrated if all observed Sr-isotopic contrasts can be satisfactorily explained by only two factors, i.e., analytical uncertainties and in situ ingrowth of ^{87}Sr.

In this paper we show that multimineral Rb/Sr internal isochrons yield valid ages for eclogitization and subsequent overprints, provided that initial isotopic equilibrium *among all phases* of a rock sample can be demonstrated.

We investigated the Eclogite Zone (EZ) of the Tauern Window in the Eastern Alps. The age of eclogite facies metamorphism is not known. Some early workers had hypothesized Late Cretaceous to Paleocene (''Eo-Alpine'') ages, while more recent publications (Zimmermann et al. 1994; Ratschbacher et al. 2004) used $^{40}Ar/^{39}Ar$ data to assign an Eocene age of between 33 Ma and ~45 Ma to the high pressure event. This would be much closer in time to the processes of Alpine nappe stacking, thermal relaxation and cooling, which have regionally been dated at ~30 Ma (Oligocene: Inger and Cliff 1994; Christensen et al. 1994). Precise age data for eclogitization are thus of considerable importance for understanding subduction/collision and exhumation processes in the Alps.

Geologic setting and metamorphic evolution

The EZ is located in the southern Tauern Window (Fig. 1). It forms a steeply S-dipping thrust sheet, tectonically sandwiched between nappes of lower metamorphic grades. Penninic crystalline basement occurs in the footwall (gneisses and parautochthonous metasediments of the venediger nappe), and a nappe stack with rocks of mainly oceanic affinity (Rote Wand-Modereck and Glockner nappes) forms the hangingwall (Fig. 1c). The EZ consists of high-pressure (HP) metasediments (carbonate-rich and graphitic schists, paragneisses, quartzites, marbles), intercalated with eclogitized mafic igneous rocks. Together, this rock sequence is interpreted as a distal succession of the passive European continental margin. The high-pressure metamorphism is inferred to be a result of the subduction of the leading edge of the European plate, culminating in continental collision with the Adriatic plate in the Paleogene (Kurz et al. 1998).

The earliest evidence of metamorphism is pre-eclogitic as documented by inclusions in garnet cores, including lawsonite pseudomorphs and glaucophane (Miller 1977; Spear and Franz 1986). The broad lithological variety of eclogite facies rocks also comprises coarse-grained metamorphic mobilisates (Holland 1979; Thomas and Franz 1988; Kurz et al. 1998). Microtextural relationships suggest that these mobilisates were formed during eclogitization and host-rock devolatilization that is syn- to post-kinematic with respect to the dominant host-rock foliation (Thomas and Franz 1988). Peak-recorded eclogite facies P–T conditions are estimated to be 2.0–2.5 GPa, 600 ± 30°C (e.g., Holland 1979; Stöckhert et al. 1997; Kurz et al. 1998; Hoschek 2001). The post-eclogitic reaction history comprises a local and incomplete blueschist facies overprint, followed by a greenschist to amphibolite facies event, regionally termed ''Tauernkristallisation'' (0.5–0.7 GPa,

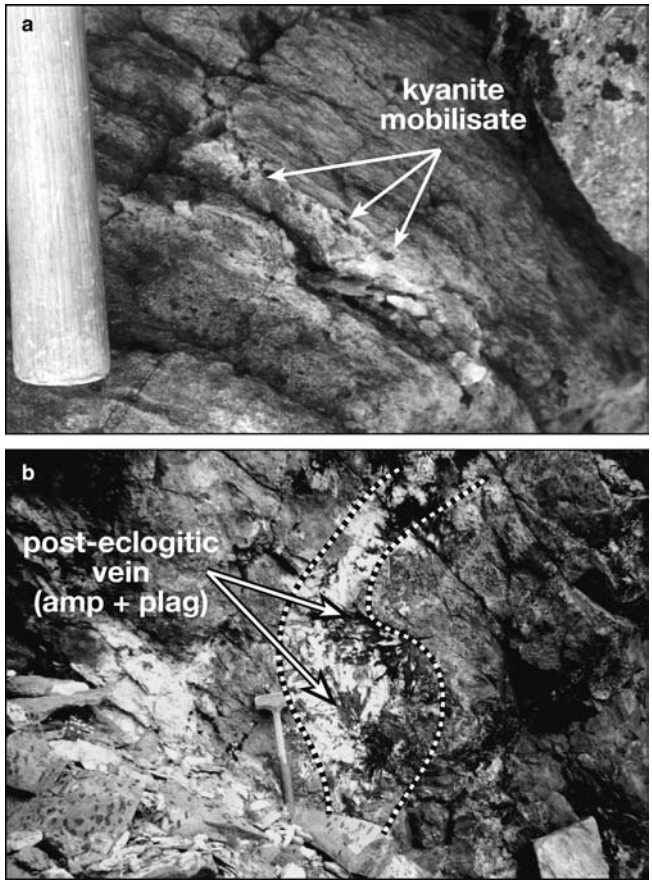

Fig. 2 **a** Sample EIS5. Eclogite facies mobilisate with cm-sized kyanite and phengite crystals, in a matrix of fine-grained eclogite. Hammer handle diameter (for scale) is 4 cm. **b** Sample EIS9. Greenschist facies, post-eclogitic vein. *Arrows* point to amphibole megacrysts (up to 15 cm), embedded in megacrystic albite. Length of hammer handle (for scale) is 35 cm

500–550°C, e.g., Dachs 1990; Selverstone 1993; Zimmermann et al. 1994). Because both foot- and hangingwall nappes lack pervasive eclogite facies metamorphism, the incorporation of the EZ into the Pennine nappe stack of the Tauern Window must postdate eclogite facies metamorphism.

Samples, sample characterization, and methodology

To isotopically date eclogite facies metamorphism, we selected five eclogite facies rocks from the western and central parts of the EZ (Timmeltal-Eisseehütte area, and Frosnitztal) for Rb/Sr mineral analysis. Sample localities and petrographic characterizations of the samples are given in the Appendix. Two of the samples were eclogite facies mobilisates (352E3 and EIS5, see Fig. 1c), which consist of up to cm-sized quartz, kyanite, and phengite crystals, with rutile and minor garnet and omphacite. Omphacite forms idiomorphic crystals in the mobilisates which suggests prograde growth at eclogite facies conditions. The mobilisates occur as local, cm- to dm-sized patches within eclogites, often elongated within the host-rock foliation (Fig. 2a). Three other samples were eclogites (EIS1, AK5-03, 291) dominated by garnet and omphacite which show slightly different assemblages and various degrees of syneclogite facies deformation and recrystallization. These samples represent carefully selected, cm-sized domains characterized by unaltered eclogitic equilibrium assemblages (Fig. 3a, a'). Post-eclogitic alteration in the sampled lithologies is non-pervasive and related to fluid infiltration, as evident from local symplectitization aureoles around fluid infiltration pathways (Fig. 3b, b'). Such aureoles are recognized macroscopically as dark-coloured veinlets within the eclogites and were cut off before sample processing. This approach ensures that only minerals

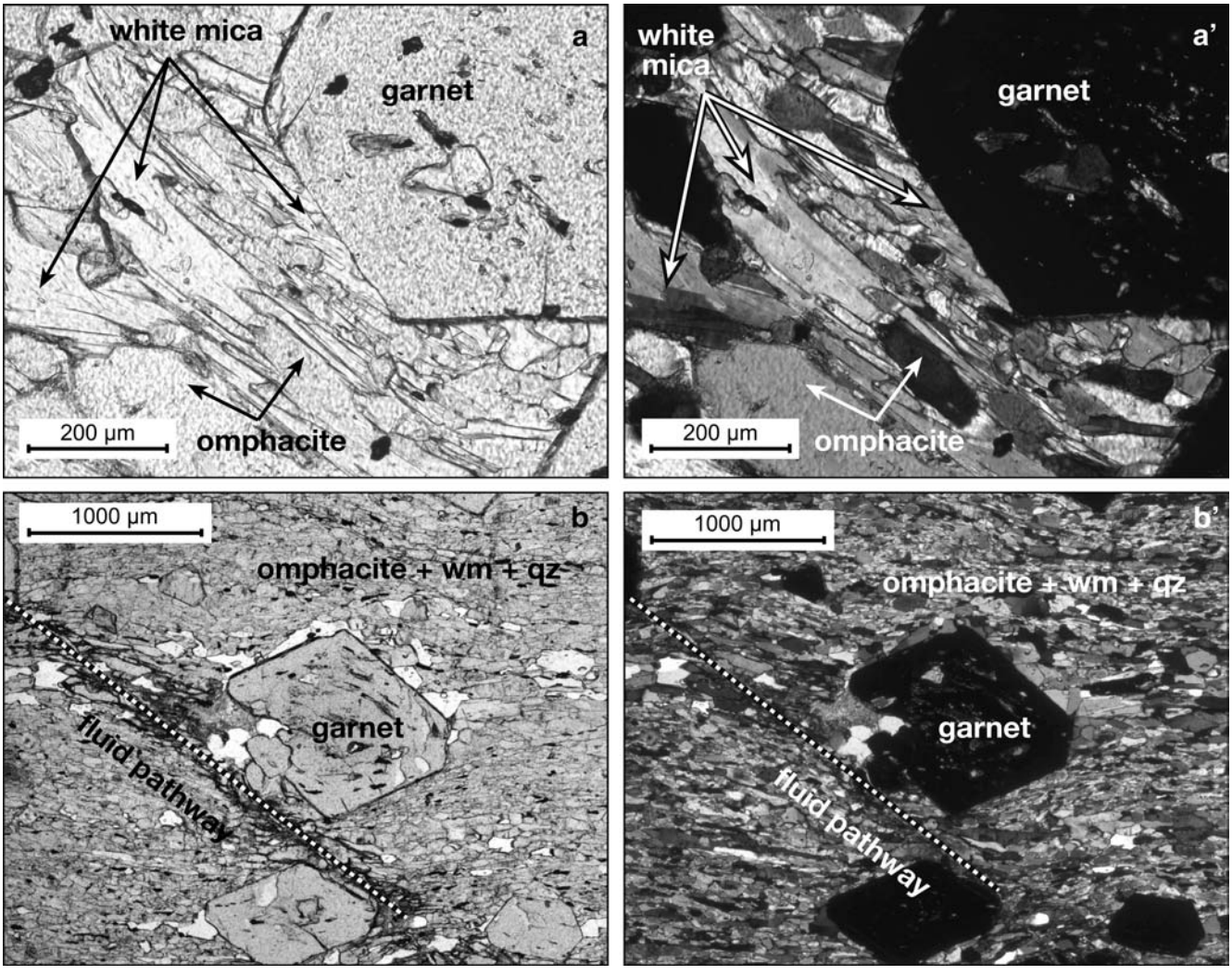

Fig. 3 Thin section micrographs (**a** and **b**, plane-polarized light; **a'** and **b'**; crossed polars) of an eclogite facies equilibrium assemblage of garnet, phengitic white mica, and omphacite; sample EIS1. Note absence of post-eclogitic mineral reaction textures in **a**. Local post-eclogitic symplectite formation along a fluid infiltration pathway is shown in **b**. Localization of retrogression proves fluid-absent conditions in the unaltered domains throughout the post-eclogitic history. Symplectite domains have been removed before further sample processing

Table 1 Mineral composition data for eclogite facies rocks of the Eclogite Zone, measured by electron microprobe

Sample	AK5-03	AK5- 03	EIS1	EIS1	EIS5	EIS5	Sample	AK5-03	AK5- 03	EIS1	EIS1	EIS5	EIS5	EIS5	Sample	AK5-03	AK5-03	EIS5	EIS5
Mineral	Omp	Omp	Omp	Omp	Omp	Omp	Mineral	Phe	Phe	Phe	Phe	Phe	Phe	Pg	Mineral	Garnet	Garnet	Garnet	Garnet
Position	Core	Rim	Core	Cim	Core	Rim	Position	Matrix	Matrix	Matrix	Matrix	Vein	Vein	Vein	Position	Core	Rim	Core	Rim
SiO_2	56.60	55.93	55.97	56.59	57.17	57.58	SiO_2	51.30	51.78	51.72	51.29	52.06	51.23	47.32	SiO_2	38.14	39.81	38.55	39.17
Al_2O_3	8.57	10.72	7.87	10.04	11.26	13.76	Al_2O_3	28.25	27.63	27.06	27.08	28.23	28.75	40.48	Al_2O_3	21.63	22.44	20.87	21.97
TiO_2	bd	0.03	0.04	0.04	0.02	0.07	TiO_2	0.24	0.22	0.31	0.32	0.18	0.24	0.04	TiO_2	0.11	0.02	0.15	0.07
Cr_2O_3	0.07	bd	0.06	0.05	0.02	0.04	Cr_2O_3	0.16	0.06	0.08	0.28	0.09	0.11	0.10	Cr_2O_3	0.07	0.09	0.02	0.09
MgO	9.54	9.11	8.72	9.01	8.49	7.55	MgO	3.88	4.13	4.03	3.98	4.02	3.82	0.23	MgO	3.03	8.85	0.94	6.05
FeO	4.91	2.67	7.56	4.53	3.42	2.14	FeO	1.26	1.16	1.78	1.83	0.94	0.94	0.24	FeO	29.16	23.48	24.34	27.51
MnO	0.04	bd	0.01	0.08	0.01	bd	MnO	bd	0.02	0.02	0.05	0.01	0.01	bd	MnO	1.15	0.41	4.23	0.32
CaO	14.36	13.72	13.64	13.93	12.69	11.18	CaO	bd	0.03	0.16	0.01	bd	0.01	0.30	CaO	7.97	6.70	12.37	6.51
Na_2O	6.26	6.59	6.73	6.49	7.53	8.42	BaO	0.30	0.34	0.03	0.27	0.31	0.14	0.07	Na_2O	bd	0.02	0.12	0.07
K_2O	0.01	bd	bd	bd	bd	0.01	Na_2O	0.86	0.63	0.53	0.49	0.86	0.90	7.08	K_2O	0.02	bd	0.02	0.03
	–	–	–	–	–	–	K_2O	9.98	10.04	10.47	10.49	9.60	9.48	0.82		–	–	–	–
Total	100.36	98.77	100.60	100.76	100.61	100.74	Cl	0.01	bd	bd	bd	bd	0.01	bd	Total	101.27	101.82	101.61	101.79
							F	bd	0.09	0.22	0.17	0.10	0.08	0.14		–	–	–	–
Si	2.01	2.00	1.99	2.00	2.00	2.00	-O eq Cl, F	0.00	0.04	0.09	0.07	0.04	0.03	0.06	Si^{4+}	5.97	5.97	6.04	5.99
Ti	0.00	0.00	0.00	0.00	0.00	0.00	Total	96.24	96.09	96.33	96.20	96.36	95.68	96.77	Al IV	0.03	0.03	0.00	0.01
Al	0.36	0.45	0.33	0.42	0.46	0.56		–	–	–	–	–	–	–	Al VI	3.96	3.93	3.85	3.95
Cr	0.00	0.00	0.00	0.00	0.00	0.00	Si	3.37	3.41	3.41	3.39	3.40	3.37	2.98	Cr	0.01	0.01	0.00	0.01
Fe total	0.15	0.08	0.23	0.13	0.10	0.06	Al IV	0.63	0.59	0.59	0.61	0.60	0.63	1.02	Fe^{3+}	0.04	0.09	0.07	0.06
Mn	0.00	0.00	0.00	0.00	0.00	0.00	Al VI	1.56	1.55	1.50	1.50	1.57	1.59	1.98	Ti	0.01	0.00	0.02	0.01
Mg	0.50	0.49	0.46	0.47	0.44	0.39	Ti	0.01	0.01	0.02	0.02	0.01	0.01	0.00	Mg	0.71	1.98	0.22	1.38
Ca	0.55	0.53	0.52	0.53	0.48	0.42	Cr	0.01	0.00	0.00	0.01	0.00	0.01	0.00	Fe^{2+}	3.78	2.85	3.12	3.46
Na	0.43	0.46	0.46	0.44	0.51	0.57	Mg	0.38	0.40	0.40	0.39	0.39	0.37	0.02	Mn	0.15	0.05	0.56	0.04
K	0.00	0.00	0.00	0.00	0.00	0.00	Fe^{2+}	0.07	0.06	0.10	0.10	0.05	0.05	0.01	Ca	1.34	1.08	2.08	1.07
	–	–	–	–	–	–	Mn	0.00	0.00	0.00	0.00	0.00	0.00	0.00		–	–	–	–
Total	4.00	4.00	4.00	4.00	4.00	4.00	Ca	0.00	0.00	0.01	0.00	0.00	0.00	0.02	Total	16.00	15.99	15.96	15.97
							Ba	0.01	0.01	0.00	0.01	0.01	0.00	0.00		–	–	–	–
Fe^{2+}	0.09	0.08	0.08	0.11	0.06	0.06	Na	0.11	0.08	0.07	0.06	0.11	0.11	0.86	Alm	63	48	52	58
Fe^{3+}	0.05	0.00	0.14	0.03	0.04	0.00	K	0.84	0.84	0.88	0.88	0.80	0.79	0.07	Adr	1	2	2	1
							Cl	0.00	0.00	0.00	0.00	0.00	0.00	0.00	Grs	21	16	33	16
Jadeite	38	45	32	42	47	56	F	0.00	0.02	0.05	0.04	0.02	0.02	0.03	Prp	12	33	4	23
Acmite	5	0	14	3	4	0	Total	6.99	6.98	7.02	7.02	6.97	6.97	7.00	Sps	2.6	0.9	9.4	0.7
Diopside	55	52	51	52	48	44		–	–	–	–	–	–	–	Uva	0.2	0.3	0.1	0.3
							Mg/Mg + Fe	0.80	0.79	0.85	0.86	0.88	0.88	0.63					
							Na/K + Na	0.07	0.07	0.12	0.09	0.12	0.13	0.93					

Omphacite: normalized to 4 cations and 6 oxygens; mica: normalized to 11 oxygens; garnet: normalized to 16 cations. *bd*, below detection limit of ~0.01%

unambiguously related to the eclogite facies history are analyzed (cf. Glodny et al. 2003).

For three of the above samples (eclogites EIS1, AK5-03, and the mobilisate sample EIS5), electron microprobe work has been carried out to constrain the reaction history of the rocks by determining mineral compositions, checking for mineral zonation, and by characterizing mineral intergrowth relationships. Quantitative mineral analysis, back-scatter electron imaging and X-ray element mapping were realized on a JEOL JXA 8900 RL superprobe at the Institut für Geowissenschaften, Universität Mainz. Natural and synthetic phases were used as standards. Mineral analyses were performed using the SilUMainz and GlimUMainz procedures with an accelerating voltage of 15 kV, a beam current of 12 nA and an electron beam of diameter 2 µm. Obtained data were corrected for absorption, atomic number, fluorescence and background using the Phi-Rho-Z method. For garnet, the almandine end-member component is defined as $Fe^{2+}/(Fe^{2+} + Mg + Mn + Ca)$. Reported values for pyrope and spessartine are calculated in a corresponding way for Mg and Mn; the andradite component is $Fe^{3+}/(Al^{VI} + Cr + Fe^{3+} + Ti)$, and grossular is given as $[Ca/(Fe^{2+} + Mg + Mn + Ca)]$-$X_{Andr}$. Ferrous and ferric iron contents in omphacite and garnet are calculated based on stoichiometric considerations. Representative mineral composition data for garnet, omphacite, and white mica (phengite, paragonite) are presented in Table 1 and plotted in Fig. 4. Mineral names are abbreviated as suggested by Kretz (1983).

Euhedral garnets from the eclogites show a complex, mostly three stage zoning pattern as indicated by the compositional trends shown in Fig. 4a. They possess almandine-rich, spessartine-enriched cores with irregular, cauliflower shaped habita and a typical composition of Alm63Grs27Prp8Sps3. Highest spessartine contents reaching 9 mol% were analyzed in garnet cores from the vein sample EIS5 (Table 1). The irregular shaped cores are surrounded by compositionally heterogeneous rims with up to 14 mol% pyrope and lower grossularite contents of down to 21 mol%, interpreted to represent a period of garnet growth during eclogite facies conditions. The outermost rim of some garnets (not shown in Fig. 4a) is a 10–15 µm thin zone with Alm45-50Grs23-24Prp22-29Sps0.5. Inclusions in garnet are numerous and consist of omphacite, epidote minerals, phengite, paragonite, quartz, kyanite and rutile. Omphacite inclusions are not found in the spessartine-enriched cores but frequently occur in the crystal rims.

Omphacite in samples EIS1 and AK5-03 is zoned with regard to its Fe_{tot}-content, with higher Fe_{tot}-contents in the core than in the rim (Fig. 4b). This correlates with an increase in jadeite component from core to rim, suggesting a prograde growth zonation. Typical core compositions are Jd37Di48-52Acm5-15, while the rims show Jd45-48Di50Acm0-3. The composition of omphacite inclusions in garnet is in the range Jd26-35Di50-52Acm20. The highest Jd-components were found in

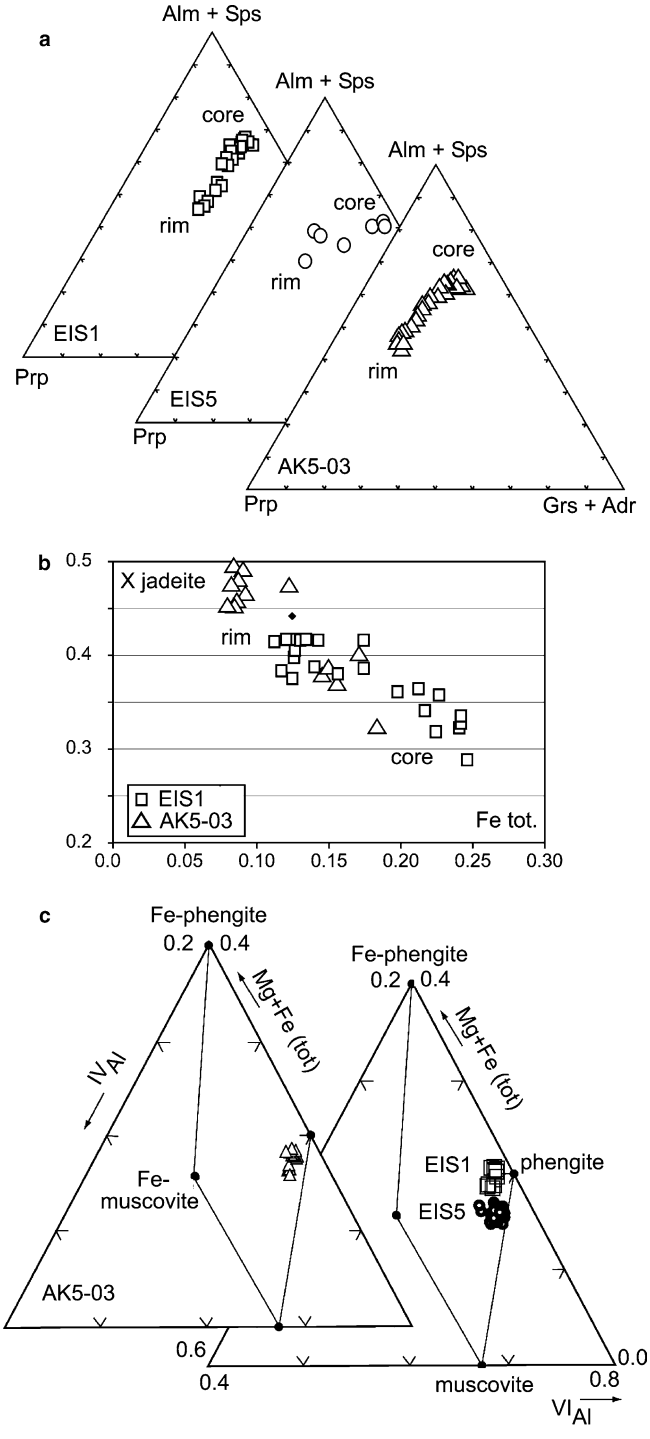

Fig. 4 **a** Composition in terms of (Alm + Sps)-Prp-(Gro + Andr) of garnets from eclogites (EIS1, AK5-03) and an eclogite facies mobilisate (EIS5). The compositional zoning is interpreted to represent garnet growth during eclogite facies conditions. **b** X_{Jd}-Fe_{tot} for omphacite from eclogite samples EIS1 and AK5-03. Note the increase in jadeite component towards the rim of the crystals. **c** Ternary composition plots for phengites from eclogites (EIS1, AK5-03) and an eclogite facies mobilisate (EIS5). All analysed phengites plot close to the phengite end-member component $[K_2(MgAl_3)(AlSi_7O_{20})(OH)_4]$ and do not show significant variations in their major element composition

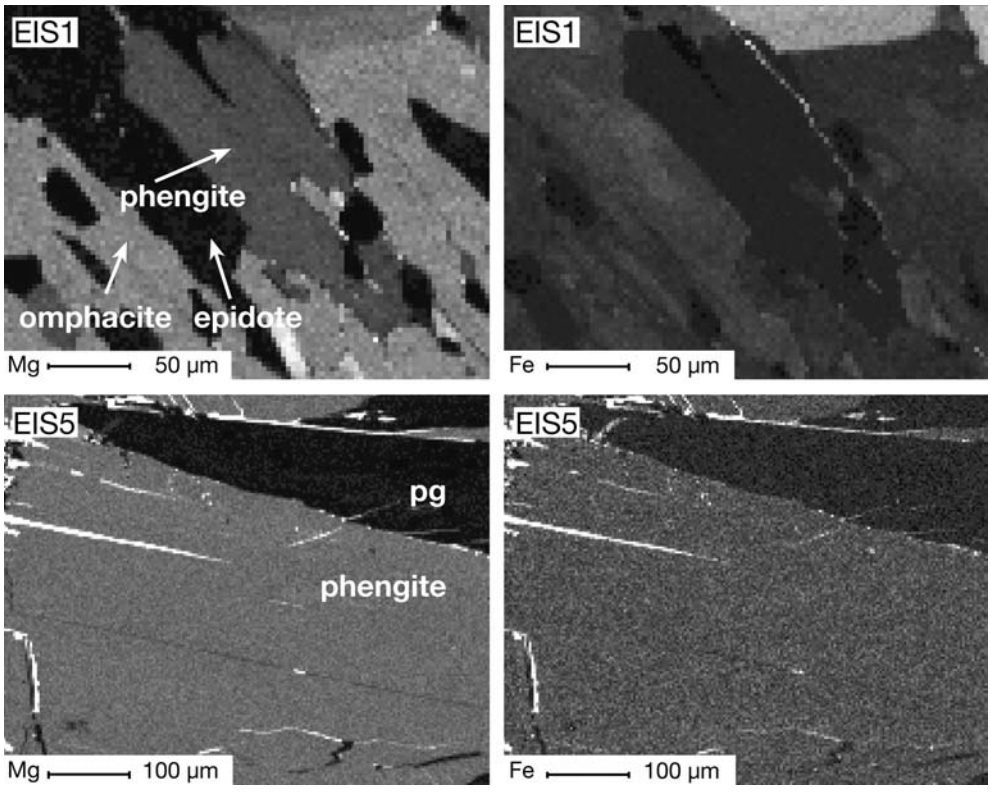

Fig. 5 X-ray maps of Mg and Fe distribution in white mica grains from the eclogite sample EIS1 (phengite) and from the eclogite facies mobilisate EIS5 (phengite + paragonite, pg). Neither phengite nor paragonite show detectable compositional zoning

omphacites from the eclogite facies mobilisate (EIS5) reaching Jd56Di44 (Table 1).

Phengite is characterized by Si-contents of ~3.4 a.p.f.u and $Mg/(Mg+Fe_{total})$ of 0.8–0.88 (Table 1), without significant variations in major element composition (Fig. 4c). X-ray maps (Fig. 5) and zoning profiles across several phengite crystals indicate absence of zoning with respect to their Mg-, Fe- and K-content. The unaltered nature of our selected samples is confirmed by complete absence of retrograde, low-Si phengites. Phengite often co-exists with paragonite (samples EIS5 and AK5-03). Similarly as phengite, paragonite shows no zoning or compositional variation (Fig. 5) and has a homogeneous Na/(Na + K) ratio of ~0.9 (Table 1).

To constrain the age of post-eclogitic overprints we investigated a structurally discordant vein mineralization (sample EIS9), which shows an aureole of greenschist facies retrogression in the eclogite, and consists of albite and actinolite/Mg-hornblende megacrysts (up to 15 cm in size) with minor titanite, rutile and muscovitic white mica (Fig. 2b). Such veins are interpreted to relate to the post-eclogitic Tauernkristallisation event (Thomas and Franz 1988).

Rb/Sr analyses were performed on all separable Sr-bearing phases of small, lithologically homogeneous rock samples (< 200 g). For white mica, we separated sub-populations with distinct magnetic properties and grain sizes, to discriminate between phengite and paragonite, and to detect possible Sr-isotopic heterogeneity. White mica fractions were ground in ethanol in an agate mortar and then sieved in ethanol to obtain inclusion free separates. Traces of secondary (Fe, Mn) hydroxides on some omphacite and garnet separates were removed with a 5% aqueous solution of oxalic acid. All mineral concentrates were checked and finally purified by hand-picking under a binocular microscope.

Rb and Sr concentrations were determined by isotope dilution using mixed ^{87}Rb–^{84}Sr spikes. Rb and Sr isotope ratios were determined on a VG-Sector 54 multicollector TIMS instrument (GeoForschungsZentrum, Potsdam) in dynamic mode. The value obtained for $^{87}Sr/^{86}Sr$ of the NBS standard SRM 987 was 0.710268 ± 0.000015 (n = 19). The observed ratios of Rb analyses were corrected for 0.25% per amu mass fractionation. Total procedural blanks were consistently below 0.15 ng for both Rb and Sr. Due to highly variable blank values, no useful blank correction was applicable. Isochron parameters were calculated using the Isoplot/Ex program of Ludwig (1999). Standard errors, as derived from replicate analyses of spiked white mica samples, of +/-0.005% for $^{87}Sr/^{86}Sr$ ratios and of +/-1.5% for Rb/Sr ratios were applied in isochron age calculations. Individual analytical errors were generally smaller than these values.

Results

For all five eclogite facies samples, statistically valid multimineral isochrons were obtained (Fig. 6, Table 2).

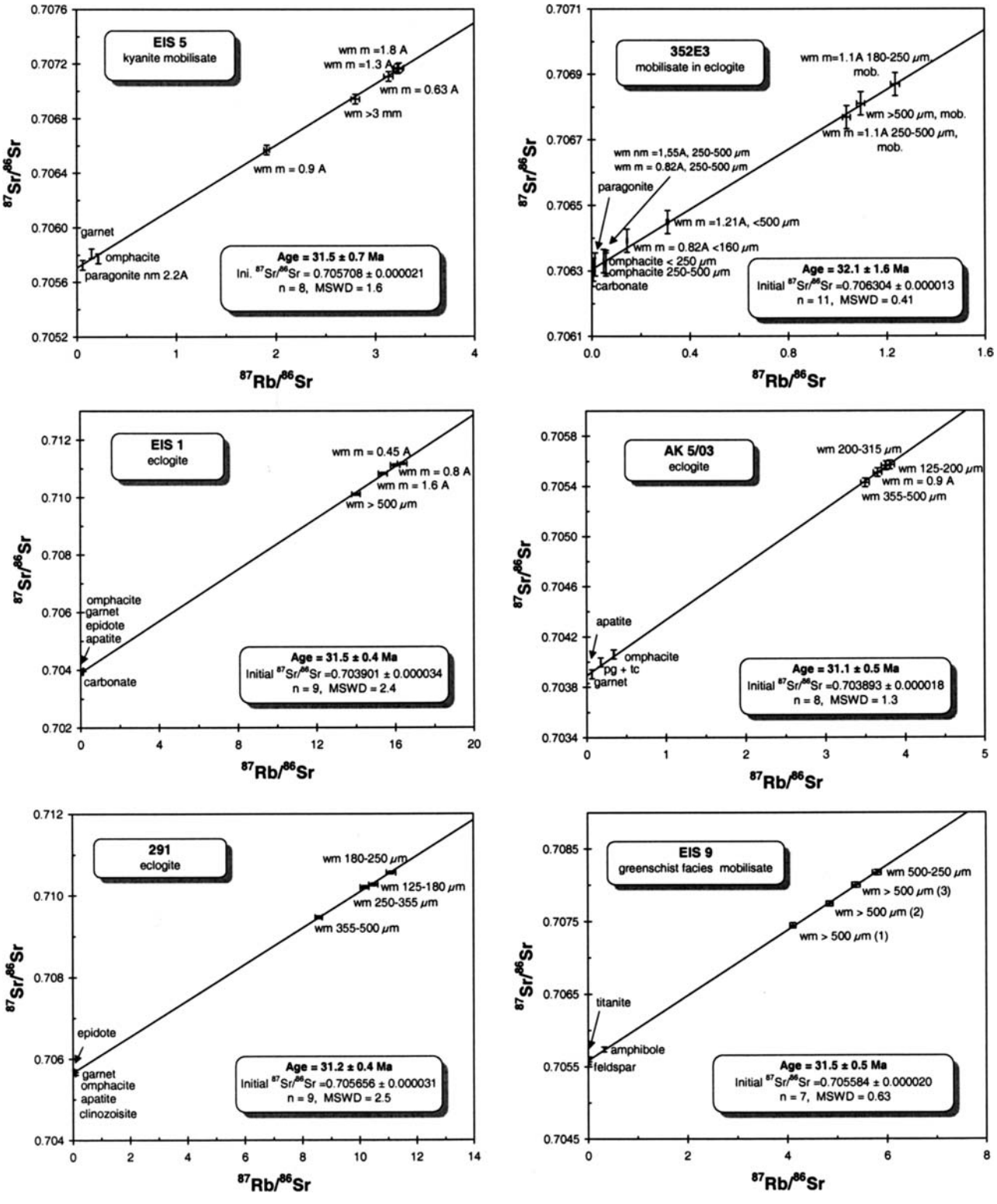

Fig. 6 Internal mineral isochrons for rocks from the Eclogite Zone, Tauern Window, Austria. Analytical data: see Table 2. Abbreviations: wm, white mica; mob, mobilisate; nm, non-magnetic; m: magnetic (Frantz magnetic separator) at 13° inclination, and electric current as indicated

Statistical validity is verified by MSWD values < 2.5 for all regression calculations (cf. Kullerud 1991). Age values for eclogite facies mobilisates and for different eclogites are identical within limits of error and give a mean age of 31.5 ± 0.7 Ma (error estimate calculated using Tukey's biweight mean).

Table 2 Rb/Sr analytical data

Sample No. Analysis No.	Material	Rb [ppm]	Sr [ppm]	$^{87}Rb/^{86}Sr$	$^{87}Sr/^{86}Sr$	$^{87}Sr/^{86}Sr$ $2\sigma_m$[%]
Eclogite facies veins						
EIS5 (31.5 ± 0.7 Ma, MSWD = 1.6, Sr_i = 0.705708 ± 0.000021)						
PS1045	Paragonite nm 2.2 A	14.1	701	0.0580	0.705726	0.0016
PS1046	Omphacite	4.59	89.8	0.148	0.705811	0.0014
PS1047	Garnet	0.86	11.6	0.215	0.705773	0.0022
PS1048	Wm m = 0.63 A	279	257	3.14	0.707106	0.0012
PS1049	Wm m = 0.9 A	195	295	1.91	0.706569	0.0014
PS1050	Wm m = 1.8 A	251	224	3.24	0.707167	0.0030
PS1056	Wm > 3 mm	256	264	2.80	0.706941	0.0012
PS1058	Wm m = 1.3 A	256	230	3.23	0.707163	0.0012
352E3 (32.1 ± 1.6 Ma, MSWD = 0.41, Sr_i = 0.706304 ± 0.000013)						
PS1018	Wm m = 0.82 A < 160 µm	101	2040	0.144	0.706392	0.0016
PS1019	Paragonite nm 2.2 A	6.15	3030	0.00586	0.706304	0.0012
PS1020	Wm nm = 1.6 A 250–500 µm	13.4	2960	0.0132	0.706320	0.0012
PS1021	Wm m = 1.21 A < 500 µm	170	1590	0.309	0.706449	0.0016
PS1022	Wm m = 0.82 A 250–500 µm	56.3	2790	0.0584	0.706327	0.0016
PS1023	Omphacite < 250 µm	3.11	187	0.0482	0.706330	0.0012
PS1024	Omphacite 250–500 µm	3.39	171	0.0574	0.706320	0.0014
PS1026	Calcite	1.28	1850	0.00199	0.706288	0.0014
PS1027	Wm[a] > 500 µm	291	768	1.10	0.706810	0.0014
PS1028	Wm[a] m = 1.1 A 180–250 µm	290	679	1.24	0.706869	0.0012
PS1052	Wm[a] m = 1.1 A 250–500 µm	286	797	1.04	0.706768	0.0014
Eclogite facies equilibrium assemblages						
EIS1 (31.5 ± 0.4 Ma, MSWD = 2.4, Sr_i = 0.703901 ± 0.000034)						
PS1011	Epidote	0.82	1550	0.00153	0.703895	0.0012
PS1013	Carbonate	0.18	494	0.00103	0.703858	0.0014
PS1014	Apatite	0.08	529	0.00042	0.703894	0.0016
PS1007	Wm m = 0.45 A	247	43.7	16.4	0.711170	0.0018
PS1008	Wm > 500 µm	243	50.1	14.0	0.710108	0.0014
PS1009	Wm m = 1.6 A	246	46.4	15.4	0.710830	0.0018
PS1010	Wm m = 0.8 A	243	43.9	16.0	0.711119	0.0016
PS1012	Omphacite	2.90	72.4	0.116	0.703989	0.0014
PS1054	Garnet	0.36	6.84	0.151	0.703994	0.0018
AK5/03 (31.1 ± 0.5 Ma, MSWD = 1.3, Sr_i = 0.703893 ± 0.000018)						
PS1100	Wm 200–315 µm	163	126	3.76	0.705563	0.0016
PS1101	Wm 125–200 µm	180	137	3.81	0.705570	0.0014
PS1102	Pg, tc, m = 2.2 A	2.72	44.8	0.176	0.703999	0.0014
PS1103	Wm 355–500 µm	106	87.3	3.50	0.705428	0.0024
PS1104	Garnet	0.20	8.71	0.0650	0.703904	0.0026
PS1105	Wm m = 0.9 A	199	158	3.66	0.705509	0.0016
PS1106	Omphacite	6.52	55.3	0.341	0.704062	0.0016
PS1107	Apatite	0.20	1370	0.00042	0.703866	0.0012
291 (31.2 ± 0.4 Ma, MSWD = 2.5, Sr_i = 0.705656 ± 0.000031)						
PS1029	Wm 0.85 A 250–355 µm	274	77.9	10.2	0.710200	0.0014
PS1030	Wm 0.85 A 125–180 µm	275	76.0	10.5	0.710263	0.0012
PS1031	Wm 0.85 A 180–250 µm	273	71.2	11.1	0.710556	0.0014
PS1032	Wm 0.85 A 355–500 µm	250	84.3	8.58	0.709464	0.0022
PS1033	Clinozoisite	4.34	4830	0.00260	0.705678	0.0014
PS1037	Apatite	0.18	1090	0.00047	0.705650	0.0014
PS1035	Omphacite	2.04	128	0.0459	0.705704	0.0014
PS1036	Epidote	3.31	5080	0.00188	0.705671	0.0012
PS1053	Garnet	0.49	14.7	0.0973	0.705640	0.0016
Greenschist facies mobilisate						
EIS9 (31.5 ± 0.5 Ma, MSWD = 0.63, Sr_i = 0.705584 ± 0.000020)						
PS1080	Feldspar	0.50	90.5	0.0159	0.705600	0.0012
PS1081	Amphibole	1.33	12.1	0.318	0.705737	0.0022
PS1077	Wm 500–250 µm	306	153	5.80	0.708170	0.0014
PS1079	Wm > 500 µm#1	292	157	5.38	0.705567	0.0014
PS1140	Wm > 500 µm#2	315	188	4.85	0.707742	0.0020
PS1141	Wm > 500 µm#3	300	211	4.12	0.707443	0.0016
PS1075	Titanite	0.18	59.6	0.00886	0.708001	0.0014

An uncertainty of ± 1.5% (2 σ) has to be assigned to Rb/Sr ratios
wm white mica, *pg* paragonite, *tc* talc
[a]Originates from mobilisate of sample 352E3. m/nm: magnetic/nonmagnetic on Frantz magnetic separator, 13° inclination, at electric current as indicated. White mica fractions of sample 352E3 are mixtures of Sr-rich paragonite with less Sr-rich phengite. Grain size of all only magnetically characterized white mica fractions is < 500 µm. Typical sample weights are 0.5–5 mg for apatite, carbonate, titanite, epidote minerals; 5–10 mg for feldspar, amphibole, white mica (paragonite and phengite), and 20–50 mg for omphacite and garnet

Rb/Sr mineral data for the post-eclogitic greenschist facies vein yield an isochron age of 31.5 ± 0.5 Ma, identical within error to the ages of the eclogite facies samples.

Discussion

Significance of the eclogite age data

The key question for interpreting the ages determined for the eclogite samples is whether they record assemblage crystallization or date a stage of subsequent cooling. Any interpretation of isotopic data in terms of cooling ages demands effective high-temperature transport of radiogenic nuclides away from their sources, which is most easily achieved in the presence of a fluid phase (Dodson, 1979). However, the EZ eclogite samples selected for this study escaped from all post-eclogitic overprints, i.e., they remained devoid of free fluids soon after assemblage crystallization, as evident from the absence of fluid-mediated retrogression reactions (Fig. 3). At such post-eclogitic fluid-absent conditions, isotope transport in the rocks is restricted to volume diffusion or grain-boundary diffusion processes, which are much less effective than transport mediated by intergranular fluids (cf. Glodny et al. 2003). In such a situation, radiogenic Sr is not lost from a rock but will, if exchanged among different phases at all, be locally redistributed. This redistribution will clearly be non-homogeneous in a rock consisting of phases with different Sr diffusivities and variable grain sizes, i.e., prolonged isotope redistribution during cooling would result in isotopic disequilibria, as modelled by Giletti (1991). In particular, diffusional escape of radiogenic Sr from white mica crystals would result in higher apparent ages for 'big' in comparison to 'small' crystals since the white mica crystals in our study generally show crystallographic continuity (Figs. 3, 5) so that Sr diffusion lengths in the mica crystals are solely determined by mica grain sizes. Such a correlation between mica grain size and Sr-isotopic composition is, however, not observed in our samples. Evidently, prolonged intermineral isotope mobility after assemblage crystallization cannot be reconciled with preservation of initial Sr-isotopic equilibria. Therefore, our valid multimineral Rb/Sr isochron ages cannot be interpreted as cooling ages.

To trace possible selective Sr isotope redistribution between white mica (the main source of radiogenic Sr) and other phases we analyzed *all* phases of the eclogitic assemblages. With this approach *all* possible sources and sinks for mobile Sr isotopes are characterized. The absence of disequilibria (Fig. 6) prove absence of isotope redistribution, and preservation of syn-eclogite facies isotopic signatures, modified only by in situ radioactive decay. We therefore interpret our statistically valid multimineral isochron ages as true crystallization ages of the eclogitic assemblages.

The studied eclogite facies *mobilisates* crystallized during prograde growth of eclogitic phases in their host rock (Thomas and Franz 1988). This is also evident from the fact that euhedral omphacite crystals grew into the quartz-kyanite-rich vein cavity (Holland 1979), and also from the general similarity in garnet zonation patterns between eclogite-facies mobilisate and eclogite samples (Fig. 4a). In a sample consisting of both a mobilisate and its matrix, we observed full initial Sr-isotopic equilibrium (sample 352E3, Table 2), in accordance with previous suggestions of mobilisate formation from fairly immobile, 'local', late-prograde devolatilization fluids (cf. Thomas and Franz 1988; Selverstone et al. 1992; Glodny et al. 2003). For the EZ *eclogites*, detailed thermobarometry has shown that maximum *P–T* estimates reflect the final increment of the prograde evolution (Holland 1979; Stöckhert et al. 1997; Kurz et al. 1998). This is in line with our finding of preservation of prograde growth zonation in omphacite and garnet in the studied samples. Since this crystallization stage, the minerals in the eclogites remained chemically virtually unchanged, as indicated by the absence of retrogression-related mineral zonation. Late-prograde element and isotope distribution patterns therefore govern both the Rb/Sr data and the petrologic *P–T* estimates. The isotopic ages, which are identical for mobilisates and eclogites, thus directly date the petrologically constrained late-prograde increments of eclogitization.

The Rb/Sr mineral isochron ages shed new light on existing $^{40}Ar/^{39}Ar$ age data from the EZ. It has previously been recognized that excess Ar is ubiquitous in amphiboles from the EZ (Zimmermann et al. 1994; Ratschbacher et al. 2004), rendering amphibole Ar–Ar ages unreliable. With an age range between 33 and 45 Ma, all published $^{40}Ar/^{39}Ar$ data for EZ white micas (cf. Zimmermann et al. 1994; Ratschbacher et al. 2004) yield significantly higher ages than obtained from Rb/Sr mineral isochrons, indicating presence of excess Ar in the white micas also. Similar problems with excess Ar in white mica and similar discrepancies between $^{40}Ar/^{39}Ar$ and Rb/Sr data have been reported from other high pressure complexes worldwide (e.g., Li et al. 1994, Arnaud and Kelley 1995, El Shazly et al. 2001). It thus appears that excess Ar is omnipresent in the EZ white mica population, that the $^{40}Ar/^{39}Ar$ dates provide only maximum ages for eclogite facies metamorphism, and that even the published statistically valid plateau ages are affected by internally undetectable excess Ar.

Sr-isotopic equilibria: petrologic implications

A striking advantage of Rb/Sr multimineral assemblage analysis is that it can be used as a petrologic tool: age information is potentially accompanied by detailed data on petrologic equilibrium–disequilibrium relationships between all Sr-bearing phases of a rock, and on metasomatic processes (cf. Molina et al. 2004). Both the presence of pre-metamorphic relics (e.g., garnet and

omphacite cores), and minute post-eclogite facies retrograde re-equilibration would be recorded, given that significant time elapsed between the different events. In our sample set, Sr-isotopic equilibrium between garnet and other eclogitic phases in all analyzed samples indicates that pre-eclogitic mineral inclusions in garnet cores relate to rapid prograde Oligocene eclogitization. Sr-isotopic equilibria between omphacite and all other eclogite facies minerals show that the observed prograde growth zonation of the omphacite is not accompanied by detectable isotopic contrasts, which suggests rapid omphacite growth. Therefore, inheritance of garnet and omphacite cores from a pre-Oligocene metamorphic event or cycle can be ruled out. Further, absence of any disequilibria among the two phases with the comparatively highest Sr diffusivities (sensu Giletti 1991; white mica, apatite) in each of the investigated rock samples points to initially rapid post-eclogitic cooling to temperatures below 500°C, where diffusional mobility of Sr within and among such phases comes to rest.

Very rapid exhumation

The analyzed greenschist facies vein from the EZ (sample EIS9) yielded a multimineral isochron age of 31.5 ± 0.5 Ma (Fig. 6), interpreted as dating crystallization. This age is identical within error to the ages obtained for the eclogitization process, and concordant with previous data on the age of the Tauernkristallisation event in the Western Tauern Window (~30 Ma, Christensen et al. 1994). Together with the 31.5 ± 0.7 Ma eclogitization age, it brackets the interval between eclogitization and the Tauernkristallisation overprint to between 32.2 and 30.8 Ma. If existing thermobarometric and geochronologic evidences are combined, more than ~50 km of exhumation (from 2.0–2.5 GPa to 0.5–0.7 GPa, i.e., from a depth of ~70–85 km to ~20 km) must have occurred in less than 1.4 Ma, which converts to a *minimum* average exhumation rate of 36 mm/a. Such a high rate equals typical subduction rates and demands extremely great slip rates on the bounding faults of > 50 mm/a (cf. Ring and Reischmann 2002). Similarly rapid exhumation seems not to be uncommon and has been reported from other high-pressure nappes in the Alps, based on different approaches. Namely for the Dora Maira eclogites (Western Alps), average exhumation rates up to 34 mm/a have been inferred, using U/Pb data of different generations of metamorphic titanite (Rubatto and Hermann 2001).

Independent evidence for very rapid exhumation also comes from Sr white mica maximum ages of up to 31 Ma for amphibolite to greenschist facies, deformed metasediments from the EZ and the overlying Glockner nappe (Inger and Cliff 1994), and also from garnet intra-crystalline diffusion patterns in an EZ-associated eclogite from the central Tauern Window, which suggests that less than 1 Ma elapsed between prograde eclogitization and cooling below 450°C, implying exhumation rates of 46–74 mm/a (Dachs and Proyer 2002). Further, Müller and Franz (2004) interpreted unusual deformation features in garnet, titanite and clinozoisite, sampled in the immediate footwall of the EZ, as recording very high strain rates, related to the 'dramatic event' of EZ emplacement within the nappe stack. In summary, the data infer that today's upper crustal nappe architecture, which includes the EZ, was established in less than 2 Ma after the eclogite facies event.

Implications for Alpine Tectonics

The new data indicate that the HP imprint on the Tauern Window Eclogite Zone occurred in the Early Oligocene, at 31.5 ± 0.7 Ma. No indications for earlier high pressure stages have been found either for an Eocene or for a Paleocene or Cretaceous ("Eo-Alpine") event. Absence of both isotopic relics and diffusion-related isotope distribution patterns rules out a hypothetic prolonged Eocene to Oligocene storage of the EZ at eclogite facies conditions. Since most recent models for Alpine collision and exhumation of Penninic nappes in the Eastern Alps currently adopt an Eocene age for the HP imprint, the new data imply that the entire Alpine evolution proceeded much more rapidly than previously assumed.

Our eclogitization age is close to (mainly U/Pb-based) eclogite facies ages of 36–32 Ma for other Penninic complexes in the Central and Western Alps (Fig. 1a; Dora Maira, Adula, and Monte Rosa complexes: Tilton et al. 1991; Dûchene et al. 1997; Gebauer 1999; Rubatto and Hermann 2001). All these complexes are interpreted as parts of the leading edge of the European passive margin. Continental collision with the Adriatic plate, the process responsible for this youngest Alpine eclogitization event, apparently occurred contemporaneously along the entire Alpine arc in the Early Oligocene. Eclogitization was immediately followed by very rapid exhumation, and by partial integration of eclogitic slices into the evolving Alpine nappe stacking processes.

There is a close temporal correlation between EZ eclogite metamorphism and regional Alpine magmatism. Entrance of continental crust into the subduction zone, as evidenced by EZ metamorphism, is likely to block the subduction process (e.g., Hynes 2002) and may lead to slab break-off. This process promotes rapid return of HP rocks to shallow depths, and instant heating of the overriding plate, with formation of partial melts (Dal Piaz and Gosso 1993; von Blanckenburg and Davies 1995). In fact, the HP event in the Eclogite Zone is contemporaneous to Alpine intrusions immediately south of the Tauern Window (Fig. 1b; Rensen pluton, 31.1–31.7 Ma, Barth et al. 1989; Rieserferner pluton, 32.4 ± 0.4 and 31.8 ± 0.4 Ma, Romer and Siegesmund 2003 and references therein).

Conclusions

Detailed analysis of minerals from eclogite facies assemblages has revealed internal Sr-isotopic equilibria from the cm- to intra-grain scales. Preservation of equilibria rules out significant post-crystallizational isotope mobility, thus indicating absence of partially reset or cooling-related signatures. We conclude that in such a situation Rb/Sr mineral data are suitable to directly date eclogite facies processes.

Our interpretation of Rb/Sr data in terms of assemblage crystallization ages is crucially dependent on initial equilibria and on proof of absence of post-crystallizational Sr-isotope mobility. This proof is achieved by analysis of *all* assemblage-forming, Sr-bearing minerals, and of white mica in different grain size fractions, as the only way to trace possible Sr-isotope redistribution. The approach of a 'system analysis' of isotope distribution is particularly well applicable to fluid-dominated systems or to fluid-precipitated mobilisates and mineralizations, in which protolith-inherited disequilibria are unlikely.

Rb/Sr assemblage analysis can verify equilibrium relationships between all Sr-bearing phases, i.e., most phases of a rock. These phases are the same as those commonly used in thermobarometry. Valid crystallization ages, assigned to unaltered equilibrium assemblages, are independent of disputable assumptions on a rock's temperature history or on isotope diffusion parameters. Therefore, this approach has a unique potential for straightforward linkage of petrology with isotopic ages, which can be employed for precisely constraining very rapid exhumation rates of deep-seated rocks.

Acknowledgements This work was supported by the Deutsche Forschungsgemeinschaft (grant RI 538/25 to UR and JG). We thank J. Herwig and V. Kuntz for their help with mineral separation and figure drawing. J. Vervoort and an anonymous referee provided helpful comments on an earlier version of this manuscript. Careful and constructive reviews by M. Bröcker and I.M. Villa are gratefully acknowledged.

Appendix

Sample characterization

EIS5 (47°04.560′N, 12°23.509′E, summit of Weißspitze mountain, 3,290 m). Eclogite facies mobilisate, very coarse-grained, dominated by kyanite + quartz + rutile + white mica. Assemblage: kyanite (cm-sized), phengite (up to several mm thick "books"), paragonite, omphacite (Fe-poor), garnet (few inclusions). Locally apatite megacrysts (up to 1 cm in length). No obvious post-eclogitic alteration phenomena.

352E3 (47°04.301′N, 12°27.071′E, Frosnitztal, 100 m SW of Steinsteg, 2,060 m). Mobilisate in matrix. Mobilisate: coarse-grained, dominated by quartz, kyanite, white mica (books up to 1 cm size), with minor amounts of carbonate, omphacite, garnet, epidote, rutile. Matrix: fine-grained eclogite, slightly foliated, with two different types of omphacite (inclusion-rich vs. inclusion-free). Assemblage: omphacite, garnet (with inclusions), with minor amounts of paragonite (rich in Sr), phengite, rutile, pyrite, zoisite, kyanite, calcite.

EIS1 (47°03.745′N, 12°23.159′E, ~100 m SE of Lake Eissee, 2,720 m). Strongly foliated eclogite, with up to 1 mm sized garnet. Locally (in pressure shadows): crystals of omphacite, epidote, and phengitic white mica up to several 100 μm in size, in an otherwise very fine-grained, omphacite + epidote-dominated matrix. Post-eclogitic alteration restricted to small domains around minute cracks (removed before analysis). Assemblage: garnet, omphacite, epidote, dolomite, apatite (Cl), phengite, paragonite, rutile, kyanite, quartz, zircon, pyrite.

AK5/03 (47°03.745′N, 12°23.159′E, ~100 m SE of Lake Eissee, 2,720 m). Eclogite, with mm-sized garnet. Few major omphacite, and phengitic white mica crystals in otherwise fine-grained, foliated, omphacite-dominated matrix. Assemblage: garnet (with inclusion-rich cores), omphacite (dominant); subordinate amounts of quartz, phengite, paragonite, talc, dolomite, epidote, rutile, ilmenite. apatite, pyrite, kyanite.

291 (47°04.799′N, 12°27.384′E, Frosnitztal, 1,150 m SW of Dabernitzkogel, 2,450 m). Fine-grained eclogite, with weakly developed foliation. Slightly weathered, with some intergranular stainings. Some small alterated domains along cracks (removed before analysis). Assemblage: garnet (with inclusion-rich cores), omphacite, clinozoisite, subordinate amounts of phengite, quartz, carbonate, rutile, epidote, apatite.

EIS9 (47°04.152′N, 12°22.603′E, 800 m SW of Wallhorntörl, 2,877 m). Vein-like, structurally discordant mobilisate, several m long and 20–50 cm wide in outcrop. Mobilisate shows 5–10 cm wide alteration aureole in wallrock, with greenschist facies overprint of eclogites. Vein assemblage: amphibole (actinolite with some Mg-hornblende; radial aggregates with crystals up to 15 cm in length), albitic feldspar megacrysts; minor amounts of muscovite (up to 5 mm diameter), titanite (poor in Fe), apatite, epidote, biotite, ilmenite. Rarity: relic of rutile, with titanite overgrowth.

References

Arnaud NO, Kelley SP (1995) Evidence for excess argon during high pressure metamorphism in the Dora Maira Massif (western Alps, Italy), using an ultra-violet laser ablation microprobe $^{40}Ar-^{39}Ar$ technique. Contrib Mineral Petrol 121:1–11

Barth S, Oberli F, Meier M (1989) U–Th–Pb systematics of morphologically characterized zircon and allanite: a high-resolution isotopic study of the Alpine Rensen pluton (northern Italy). Earth Planet Sci Lett 95:235–254

von Blanckenburg F, Davies JH (1995) Slab breakoff: A model for syncollisional magmatism and tectonics in the Alps. Tectonics 14(1):120–131

Blichert-Toft J, Frei R (2001) Complex Sm–Nd and Lu–Hf isotope systematics in metamorphic garnets from the Isua supracrustal belt, West Greenland. Geochim Cosmochim Acta 65(18):3177–3189

Christensen JN, Selverstone J, Rosenfeld JL, DePaolo DJ (1994) Correlation by Rb–Sr geochronology of garnet growth histories from different structural levels within the Tauern Window, Eastern Alps. Contrib Mineral Petrol 118:1–12

Cliff RA, Meffan-Main S (2003) Evidence from Rb–Sr microsampling geochronology for the timing of Alpine deformation in the Sonnblick Dome, SE Tauern Window, Austria. In: Vance D, Mueller W, Villa IM (eds) Geochronology: linking the isotopic record with petrology and textures. Geol Soc Spec Pub 220:159–172

Dachs E (1990) Geothermobarometry in metasediments of the southern Grossvenediger area (Tauern Window, Austria). J Metam Geol 8:217–230

Dachs E, Proyer A (2002) Constraints on the duration of high-pressure metamorphism in the Tauern Window from diffusion modelling of discontinuous growth zones in eclogite garnet. J Metam Geol 20:769–780

Dal Piaz GV, Gosso G (1993) Some remarks on evolution of the Alpine lithosphere. In: Proceedings of symposium "CROP—Central Alps", Sondrio, pp 93–101

Dodson MH (1973) Closure temperature in cooling geochronological and petrological systems. Contrib Mineral Petrol 40:259–274

Dodson MH (1979) Theory of cooling ages. In: Jaeger E, Hunziker JC (eds) Lectures in isotope geology. Springer Berlin Heidelberg New York, pp 194–202

Dûchene S, Blichert-Toft J, Luais B, Télouk P, Lardeaux J-M, Albarède F (1997) The Lu-Hf dating of garnets and the ages of the Alpine high-pressure metamorphism. Nature 387(6633):586–589

El-Shazly AK, Bröcker M, Hacker B, Calvert A (2001) Formation and exhumation of blueschists and eclogites from NE Oman: new perspectives from Rb–Sr and $^{40}Ar/^{39}Ar$ dating. J Metam Geol 19:233–248

Frisch W, Dunkl I, Kuhlemann J (2000) Post-collisional orogen-parallel large-scale extension in the Eastern Alps. Tectonophysics 327:239–265

Gebauer D (1999) Alpine geochronology of the Central and Western Alps: new constraints for a complex geodynamic evolution. Schweiz Mineral Petrogr Mitt 79:191–208

Giletti BJ (1991) Rb and Sr diffusion in alkali feldspars, with implications for cooling histories of rocks. Geochim Cosmochim Acta 55:1331–1343

Glodny J, Austrheim H, Molina JF, Rusin A, Seward D (2003) Rb/Sr record of fluid-rock interaction in eclogites: the Marun-Keu complex, Polar Urals, Russia. Geochim Cosmochim Acta 67(22):4353–4371

Holland TJB (1979) High water activities in the generation of high pressure kyanite eclogites of the Tauern Window, Austria. J Geol 87(1):1–27

Hoschek G (2001) Thermobarometry of metasediments and metabasites from the Eclogite Zone of the Hohe Tauern, Eastern Alps, Austria. Lithos 59:127–150

Hynes A (2002) Encouraging the extrusion of deep-crustal rocks in collision zones. Mineralogical Magazine 66(1):5–24

Inger S, Cliff RA (1994) Timing of metamorphism in the Tauern Window, Eastern Alps: Rb-Sr ages and fabric formation. J Metam Geol 12:695–707

Jahn B, Caby R, Monie P (2001) The oldest UHP eclogites of the World: age of UHP metamorphism, nature of protoliths and tectonic implications. Chemical Geol 178:143–158

Jenkin GRT, Ellam RM, Rogers G, Stuart FM (2001) An investigation of closure temperature of the biotite Rb/Sr system: the importance of cation exchange. Geochim Cosmochim Acta 65(7):1141–1160

Kelley SP, Wartho JA (2000) Rapid kimberlite ascent and the significance of Ar–Ar ages in xenolith phlogopites. Science 289(5479):609–611

Kretz R (1983) Symbols for rock-forming minerals. Am Mineral 68:277–279

Kühn A, Glodny J, Iden K, Austrheim H (2000) Retention of Precambrian Rb/Sr ages through Caledonian eclogite facies metamorphism, Bergen Arc Complex, W-Norway. Lithos 51:305–330

Kullerud L (1991) On the calculation of isochrons. Chemical Geol 87:115–124

Kurz W, Neubauer F, Dachs E, (1998) Eclogite meso-and microfabrics: implications for the burial and exhumation history of eclogites in the Tauern window (Eastern Alps) from *P–T–d* paths. Tectonophysics 285:183–209

Li S, Wang S, Chen Y, Liu D, Ji Q, Zhou H, Zhang Z (1994) Excess argon in phengite from eclogite; evidence from dating of eclogite minerals by Sm–Nd, Rb–Sr and $^{40}Ar/^{39}Ar$ methods. Chemical Geol 112(3–4):343–350

Ludwig KR (1999) Isoplot/Ex Ver 2.06: a geochronological toolkit for Microsoft Excel. Berkeley Geochronology Center Special Publications 1a.

Meffan-Main S, Cliff RA, Barnicoat AC, Lombardo B, Compagnoni R (2004) A Tertiary age for Alpine high-pressure metamorphism in the Gran Paradiso massif, Western Alps: a Rb–Sr microsampling study. J Metam Geol 22(4):267–281

Miller C (1977) Chemismus und phasenpetrologische Untersuchungen der Gesteine aus der Eklogitzone des Tauernfensters, Österreich. Tschermaks Min Petr Mitt 24:221–277

Molina JF, Poli S, Austrheim H, Glodny J, Rusin A (2004) Eclogite-facies vein systems in the Marun-Keu complex (Polar Urals, Russia): textural, chemical and thermal constraints for patterns of fluid flow in the lower crust. Contrib Mineral Petrol 147(4):484–504

Müller W (2003) Strengthening the link between geochronology, textures and petrology. Earth Planet Sci Lett 206:237–251

Müller WF, Franz G (2004) Unusual deformation microstructures in garnet, titanite and clinozoisite from an eclogite of the Lower Schist Cover, Tauern Window, Austria. Eur J Mineral 16:939–944

Raith M, Mehrens C, Thöle W (1980) Gliederung, tektonischer Bau und metamorphe Entwicklung der penninischen Serien im südlichen Venediger-Gebiet, Osttirol. Jahrbuch der Geol Bundesanstalt 123(1):1–37

Ratschbacher L, Dingeldey C, Miller C, Hacker BR, McWilliams MO (2004) Formation, subduction, and exhumation of Pennic oceanic crust in the Eastern Alps: time constraints from $^{40}Ar/^{39}Ar$ geochronology. Tectonophysics 394:155–170

Ring U, Reischmann T (2002) The weak and superfast Cretan detachment, Greece: exhumation at subduction rates in extrusion wedges. J Geol Soc London 159:225–228

Romer RL, Siegesmund S (2003) Why allanite may swindle about its true age. Contrib Mineral Petrol 146:297–307

Rubatto D, Hermann J (2001) Exhumation as fast as subduction? Geology 29(1):3–6

Selverstone J (1993) Micro- to macroscale interactions between deformational and metamorphic processes, Tauern Window, Eastern Alps. Schweiz Min Pet Mitt 73:229–239

Selverstone J, Franz G, Thomas S, Getty S (1992) Fluid variability in 2 GPa eclogites as an indicator of fluid behaviour during subduction. Contrib Mineral Petrol 112:341–357

Spear FS, Franz G (1986) *P–T* evolution of metasediments from the Eclogite Zone, south-central Tauern Window, Austria. Lithos 9:219–234

Stöckhert B, Massonne H-J, Nowlan EU (1997) Low differential stress during high-pressure metamorphism: the microstructural record of a metapelite from the Eclogite Zone, Tauern Window, Eastern Alps. Lithos 41:103–118

Thomas S, Franz G (1988) Kluftminerale und ihre Bildungsbedingungen in Gesteinen der Eklogitzone/Südvenediger-Gebiet (Hohe Tauern, Österreich) Mitteilungen der Österreichischen Geologischen Gesellschaft 81:189–218

Thöni M, Jagoutz E (1992) Some new aspects of dating eclogites in orogenic belts: Sm–Nd, Rb–Sr, and Pb–Pb results from the Austroalpine Saualpe and Koralpe type-locality (Carinthia/Styria, SE Austria). Geochim Cosmochim Acta 56:347–368

Tilton GR, Schreyer W, Schertl H-P (1991) Pb-Sr-Nd isotopic behaviour of deeply subducted crustal rocks from the Dora Maira massif, Western Alps, Italy—II: what is the age of the ultrahigh-pressure metamorphism? Contrib Mineral Petrol 108:22–33

Vance D, Müller W, Villa IM (eds) (2003) Geochronology: linking the isotopic record with petrology and textures. Geol Soc Lond Spec Publ 220:1–260

Villa IM (1998) Isotopic closure. Terra Nova 10:42–47

Zimmermann R, Hammerschmidt K, Franz G (1994) Eocene high pressure metamorphism in the Penninic units of the Tauern Window (Eastern Alps): evidence from ^{40}Ar–^{39}Ar dating and petrological investigations. Contrib Mineral Petrol 117:175–186